Preferred nanocrystalline configurations in ternary and multicomponent alloys

Citation: Xing, Wenting, Arvind R. Kalidindi, and Christopher A. Schuh. "Preferred Nanocrystalline Configurations in Ternary and Multicomponent Alloys." Scripta Materialia 127 (January 2017): 136–140. doi:10.1016/j.scriptamat.2016.09.014.

As Published: https://doi.org/10.1016/j.scriptamat.2016.09.014

Publisher: Elsevier

Persistent URL: http://hdl.handle.net/1721.1/120334

Version: Author's final manuscript: final author's manuscript post peer review, without publisher's formatting or copy editing

Preferred Nanocrystalline Configurations in Ternary and Multicomponent Alloys

Wenting Xing, Arvind R. Kalidindi, *Christopher A. Schuh**

Department of Materials Science and Engineering, Massachusetts Institute of Technology, 77 Massachusetts Avenue, Cambridge, Massachusetts 02139, USA

KEYWORDS Ternary alloys, Grain boundary segregation, Nanostructure stability, Monte Carlo

ABSTRACT

In nanocrystalline alloys, a range of configurations can have low energies when solute atoms have favorable interactions with interfaces. Whereas binary nanostructured alloys have been well studied, here we lay groundwork for the computational thermodynamic exploration of alloy configurations in multicomponent nanocrystalline alloys. Multicomponent nanostructured systems are shown to occupy a vast space, with many topological possibilities not accessible in binary systems, and where the large majority of interesting configurations will be missed by a regular solution approximation. We explore one interesting ternary case in which the first alloying element stabilizes grain boundaries, and the second forms nano-sized precipitates.

Graphical abstract (required)

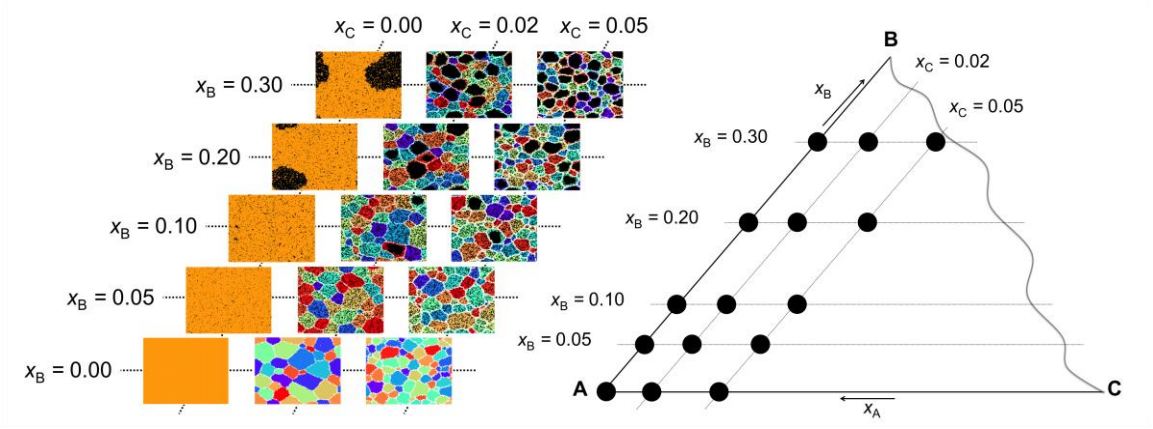

Reducing grain size into the nanoscale regime is a promising pathway to improve the properties of engineering materials, such as achieving a high figure of merit in thermoelectric materials [1–3], improving the coercivity of magnets [4–6], and reaching superior mechanical properties such as high strength and wear resistance [7–11]. Attaining and retaining grain sizes in the nanoscale regime, however, is contrary to the normal tendency for rapid grain growth when such a large volume fraction of grain boundaries is present. Stabilizing nanostructure is generally most plausible in alloyed systems, where, e.g., an alloying element that exhibits a strong preference for grain boundary sites is introduced [12–23]. In such an alloy system, grain growth is not just kinetically impeded, but can be thermodynamically unfavorable if the dissolution of the segregant into the crystal lattice is an energy-raising proposition.

The role of the spatial distribution of alloying elements (i.e. the alloy configuration) on the stability of nanostructured systems has been widely studied in binary alloys, using a variety of approaches that include ideal solution, regular solution, or other configurational assumptions [24–30]. The lattice Monte Carlo approach of Chookajorn and Schuh [28] permitted a more stochastic approach to alloy configuration without enforcing ideality or regularity, and produced a similar set of predictions. This included the identification of four different classes of stable binary states in positive enthalpy of mixing systems: a grain boundary segregated state, a duplex state with both grain boundary segregation and solute precipitation, a state with no grain boundary segregation but with solute precipitation, and a bulk state with phase separation. The nanocrystalline states are not predictable from a bulk phase diagram, but result from the

possibility that the solute atoms can segregate to grain boundaries and attain a different energetic state than in any bulk phase.

In ternary alloys where interface states are allowed, the number of different accessible nanostructure configurations is expected to be substantially larger, because the topological complexity available with three species is much higher, and the two solute elements can have additional interactions that lead to nontrivial configurations. Consider, as an example, an alloy characterized by simple nearest-neighbor pairwise interactions among elements A, B, and C. If the neighbor pairs are also subclassified as either crystalline (superscript 'c') or grain boundary (superscript 'gb') bonds, then a binary system would have six different bond energies, E_{AA}^{c}, E_{BB}^{c}, E_{AB}^{c}, E_{AA}^{gb}, E_{BB}^{gb} and E_{AB}^{gb}, while a ternary one would require those plus an additional six, E_{CC}^{c}, E_{AC}^{c}, E_{BC}^{c}, E_{CC}^{gb}, E_{AC}^{gb}, E_{BC}^{gb}. Since the relative magnitudes of these energies should determine the equilibrium configuration, the addition of more terms leads to an even more drastic increase in the number of relative orderings of the energies they represent. In general a total of $n(n+1)$ bonds in an *n*-ary nanocrystalline alloy system result in a total of $[n(n+1)]!$ different bond energy orderings, and by extension unique configurational classes. Applying the constraint that the like-atom grain boundary bonds should always have a higher energy than the like-atom crystalline bonds, we estimate that a maximum of $\frac{[n(n+1)]!}{2^n}$ different alloy configuration classes exist in nanostructured *n*-ary alloys.

The black circular data points in Figure 1 show the consequence of this scaling for *n*-ary alloys; we immediately see that the ternary problem in nanocrystalline alloys is many orders of magnitude more complicated than the binary problem, in the number of

nominally distinct system configurations that are achievable. On the other hand, we may also expect some significant degeneracy amongst these states; in any given ordering of the bond energies we might imagine that only the lowest ones are relevant to the equilibrium structure, and higher energies will correspond only to activated states that are rarely, if ever, sampled, and only when entropy or geometric constraints from other elements are important. For example, the four clearly distinct configurations reported by Chookajorn and Schuh in the binary alloy model were dictated by only the two lowest bond energies for each element [28], as compared to the nominal ~200 predicted in Figure 1. If we limit our discussion to the number of orderings of the *r* lowest-energy bonds for each element in the system (*r* denoting the "rank" of the bond orders considered), the number of states is considerably reduced. This is also shown in Figure 1, where we count the number of subsets of size *r* of the bond energy set, and all permutations within those subsets under the constraint that $E^{gb} > E^{c}$ for like-atom bonds of all elements.

An algorithm that enumerates the number of distinct bond orderings is provided in the Supplementary Material, and the results of such calculations are shown for different ranks in Figure 1. As expected, focusing attention on the most energetically favorable terms reduces the number of possible distinct nanostructured alloy configurations dramatically. However, the main point remains: the ternary problem is more than an order of magnitude more complicated than the binary one in any case, and adding components to the problem raises the number of possible configurations exponentially. Of the 2,016 different combinations in the 2nd rank ternary model, 1,854 could be nanocrystalline states (i.e. at least one of the two lowest-energy bonds of an element is a

grain boundary bond), and thus a large space of interesting nanostructures may exist as thermodynamic equilibrium states that have yet to be explored.

On the other hand, we can consider the number of distinct nanostructural configurations that may be achieved under the regular solution assumption, i.e., forced random mixing. The regular solution assumption only allows for grain boundary segregation and solid solution states, and does not permit ordering; it therefore can address only very few configurations compared to an unconstrained system. So far as we are aware, the only works considering multinary nanostructured systems have relied on this simplifying assumption [27] or an even stricter assumption of ideal solution behavior [23], but in addition to being physically questionable, we see in Figure 1 that the regular solution simplification misses much of the interesting complexity in multinary systems. Hundreds or thousands of distinct configurations are possible when mixing is permitted to be nonrandom, and we expect that this is the most interesting space for investigation of ternary nanostructured alloys.

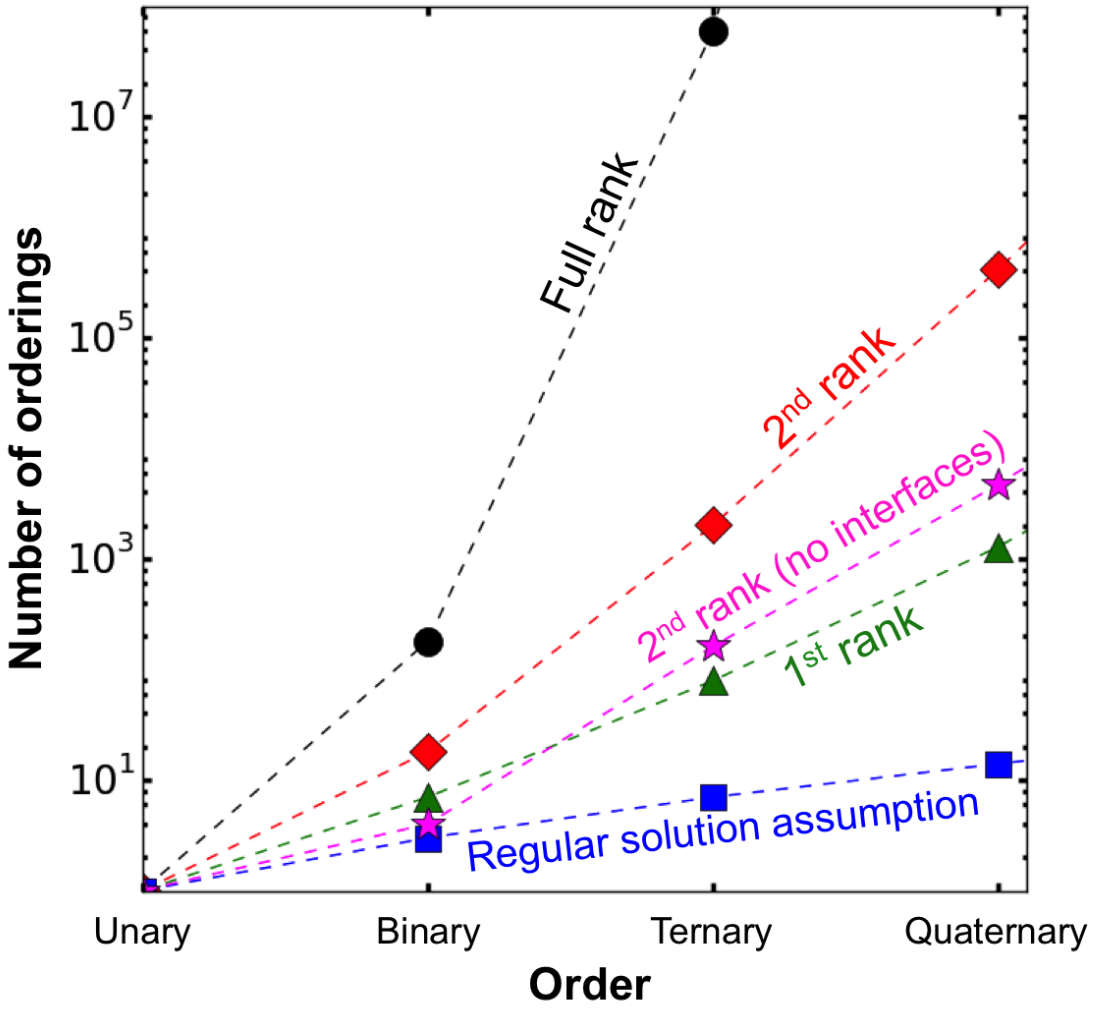

Figure 1. The number of distinct alloy configuration classes based on the number of alloying elements in the system. This is calculated considering all pairwise bond energies (full rank), and also considering only the lowest 'r' bond energies (rank 'r').

The results in Figure 1 motivate greater study of ternary and multinary nanostructured alloys, and imply a rich array of alloy configurations that could be of

scientific and technological value. However, they also show that the space of possibilities is vast and complicated, so thermodynamic methodologies that can both rapidly scan the space while capturing the most essential physical features and avoiding the most limiting assumptions are needed to address this problem. We propose that lattice Monte Carlo simulations of the kind first proposed by Chookajorn and Schuh [28] and applied to a number of binary systems [31–35] may contribute to the rapid assessment of the ternary and multinary alloy configuration space. Rather than address the entire space in the present letter, we take a first step to illustrate the opportunities for alloy design in nanostructured ternary alloys. We perform a case study where the majority solute (B) prefers a bulk, phase separated microstructure and anti-segregates from grain boundaries in the solvent (A), while the minority solute (C) has a strong preference for grain boundary segregation and prefers a nanocrystalline state. Accordingly, the bond energy order chosen is:

$$E_{AB}^{gb} > E_{BC}^{gb} > E_{CC}^{gb} > E_{AA/BB}^{gb} > E_{AC/BC}^{c} > E_{CC}^{c} > E_{AB}^{c} > E_{AA/BB}^{c} > E_{AC}^{gb} \quad (1)$$

The bond energies can be related to actual alloy systems according to the enthalpy of mixing and enthalpy of grain boundary segregation for each element pair, as per the method in Ref. [28], where increasing the enthalpy of grain boundary segregation of an element pair generally leads to a decrease in the corresponding grain boundary pairwise bond energy and increasing the enthalpy of mixing leads to an increase in the corresponding crystalline pairwise bond energy. Here, the bond energies (shown in Table 1) are chosen to reflect enthalpies of mixing of $\Delta H_{AB}^{mix} = \Delta H_{AC}^{mix} = \Delta H_{BC}^{mix} = 20 {}^{kJ}\!/_{mol}$ and

enthalpies of grain boundary segregation of $\Delta H_{AB}^{seg} = -45 \, kJ/mol$, $\Delta H_{AC}^{seg} = 65 \, kJ/mol$, and $\Delta H_{BC}^{seg} = 10 \, kJ/mol$.

Table 1. Bond energies for corresponding simulations

Corresponding Figures	Bond Energy [meV/bond]								
	$E_{AA/BB}^{c}$	E_{CC}^{c}	E_{AB}^{c}	$E_{AC/BC}^{c}$	$E_{AA/BB}^{gb}$	E_{CC}^{gb}	E_{AB}^{gb}	E_{AC}^{gb}	E_{BC}^{gb}
Fig. 2, Fig. 3(c)	0	31.2	25.9	41.5	50	81.2	218.4	-51	91.5
Fig. 3(a)	0	31.2	25.9	41.5	50	81.2	218.4	62.9	91.5
Fig. 3(b)	0	31.2	-25.9	41.5	50	81.2	114.7	-51	91.5
Fig. 3(d)	0	31.2	25.9	41.5	50	81.2	44.8	-51	91.5

We use the Monte Carlo method of Chookajorn and Schuh [28] to identify the equilibrium alloy configuration of this system. In this approach, each lattice site has a chemical identity – either an A, B, or C atom – and a grain number such that adjacent lattice sites with different grain numbers have a grain boundary pairwise bond energy. Two Monte Carlo events are used to explore the configuration space of this alloy: an atom swap where two different types of atoms are randomly swapped and a grain swap where the lattice sites at the grain boundary can change their grain number to that of an adjacent grain or take on an entirely new grain number. For this study, compound forming alloys are not considered in order to avoid the need for compound units and multi-body interactions [36]. Starting from a very high temperature of 10,000K and slowly lowering it to 773K through 100,000 Monte Carlo steps, the simulation equilibrates at the lowest free energy alloy configuration considering both nanocrystalline and single crystalline alloy configurations on a 200x200x6 BCC lattice. Although the simulations are three dimensional, we show two dimensional cut sections throughout the

paper. The Python code for this simulation is provided in the Supplementary Material and for more details the reader is referred to the original work of Chookajorn and Schuh [28].

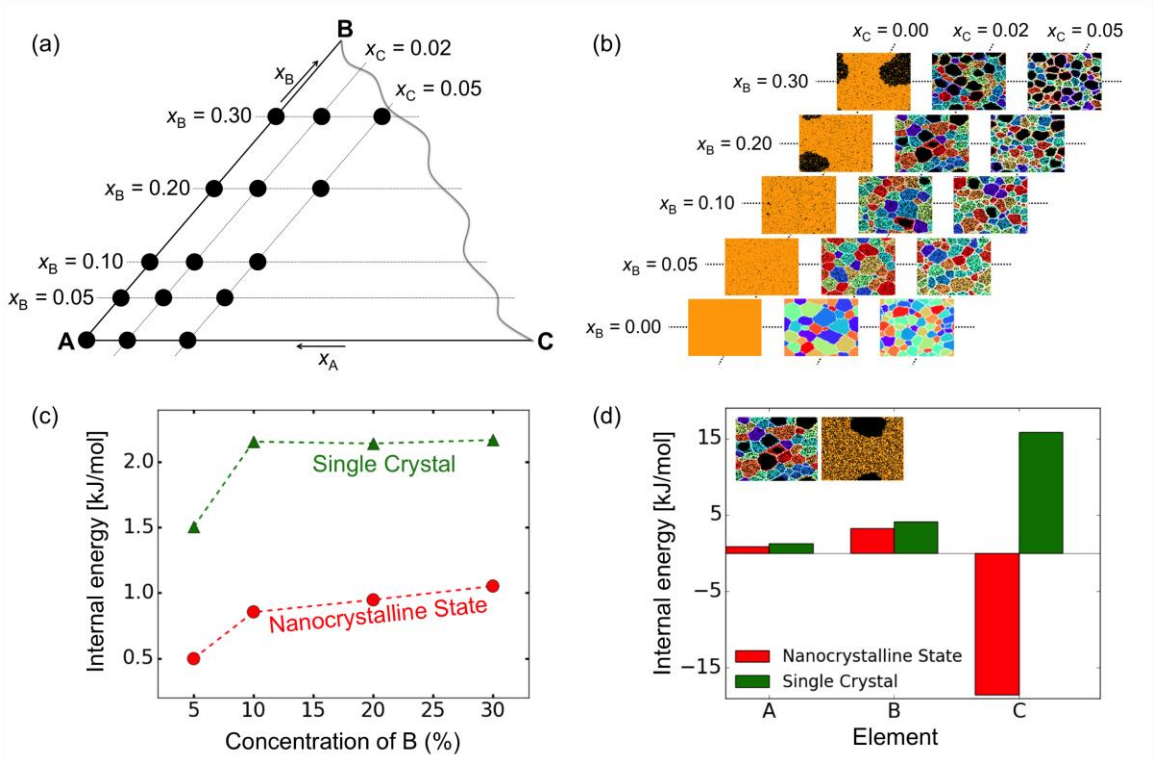

Figure 2. **(a)** A schematic of the solvent-rich portion of the ternary composition space with **(b)** corresponding equilibrated nanostructures (B atoms in black, C atoms in white, and colors denote different grain allegiance). **(c)** The internal energy of equilibrated nanostructured states (2 at.% C atoms) are compared to equilibrated single crystal states at different concentrations of B; **(d)** the internal energies are broken down to each element for the 20 at.% B and 2 at.% C alloy.

Figure 2a shows the solvent-rich corner of the ternary phase diagram under consideration, along with a series of nanostructures equilibrated at 500°C at a variety of

compositions in Figure 2b. The A-B binary edge of this system has a bulk, phase separated ground state, and at 500°C exhibits solubility of B in A to a saturation limit around 5 at.%. Conversely, the A-C binary edge evolves a grain boundary segregated nanocrystalline state, wherein smaller average grain sizes are stabilized with increasing amounts of solute C. This behavior is denoted by Chookajorn and Schuh [28] as a "classical nanostructure" and is the most well-studied case of a grain boundary segregation-stabilized nanostructure in the literature.

In the ternary alloy, the binary A-B and A-C states appear to roughly superimpose; the equilibrated states that emerge in Fig. 2b all exhibit grain boundaries decorated with C and B-rich precipitates. In fact, the equilibrium grain size is apparently prescribed by the concentration of C, declining in a manner similar to that seen in the A-C binary system and essentially independent of the amount of B. However, the C-enforced nanocrystalline state disrupts the tendency for B to aggregate into a single precipitate as favored by the bulk thermodynamics of the A-B binary. Instead, element B forms nano-precipitates within nano-grains defined by C-rich boundaries. Due to the grain boundary anti-segregating tendency of B, a core-shell structure within the grains forms with the region of A atoms separating the precipitate of B atoms from the grain boundary which is saturated with C atoms (shown more clearly in Figure 3c).

The energetic preference for a nanostructured state in this ternary alloy is confirmed by comparing the internal energy of this structure with that of an equilibrated structure in a single crystal as shown in Figure 2 (c-d). The single crystal reference state is assessed at the same composition by equilibrating a structure in which interfacial states are not allowed and a single grain number is enforced over the whole structure. Overall, it

is clear that the system favors the formation of a nanostructured state due to the substantial energetic benefit for C atoms to reside at grain boundary sites. It is further noted that all elements receive an energetic benefit from forming the nanostructure in this case: since C atoms are no longer dissolved in the A matrix, A atoms see an energetic relief; and B atoms, though forced to form a number of nano-precipitates instead of one coarsened precipitate, form a larger total volume of B precipitate, which lowers the internal energy of B. The increase in precipitation is attributed to the unique core shell grain structure, where 15% of the lattice sites are occupied by grain boundary atoms. As a result, B atoms are only able to occupy 85% of the system, which increases the effective supersaturation of B, leading to more precipitation. In addition, although solute C prefers to segregate to the grain boundaries and solute B prefers anti-segregation, we do not find that the presence of B negates the energy reduction of the grain boundaries of A due to the presence of C, as has been previously expected analytically [6] based on a regular solution assumption. This is due to the independence of B and C and their ability to locally order in non-regular arrangements that are energy lowering.

In terms of the bond energy framework, the lowest two bond energies for each element largely dictate the formation of the duplex grain structure in Fig. 2(b). Specifically, C atoms at grain boundaries are preferred by $E_{AC}^{gb} < E_{AA}^{c}$ (for A) and $E_{AC}^{gb} < E_{CC}^{c}$ (for C) whereas second phase B precipitation is favored by $E_{BB}^{c} < E_{AB}^{c}$ (for B). Different possible 2nd rank orders will, in most cases, produce different equilibrium configurations; for instance,

a. when the two lowest bond energies for A and C are crystalline with a tendency to phase separate – $E_{AA}^{c} < E_{AC}^{c}$ and $E_{CC}^{c} < E_{AC}^{c}$ – a nanocrystalline state is no longer the minimum free energy configuration and bulk thermodynamics prevails.
b. when the lowest bond energies for B are reversed to be $E_{AB}^{c} < E_{BB}^{c}$, solute precipitates of B no longer form.

These two cases are respectively shown explicitly in Fig. 3(a) and (b), where ΔH_{AC}^{seg} is lowered to $21 kJ/mol$ for the first case and ΔH_{AB}^{mix} is lowered to $-20 kJ/mol$ for the second, with all other thermodynamic parameters maintained from the simulations in Fig. 2 (corresponding bond energies shown in Table 1).

However, considering all 2nd rank orders in this alloy is not necessarily sufficient either, and one such case is shown in Figure 3(c-d). The microstructure in Figure 3(c) is the same as the one in Figure 2 ($x_B = 0.2, x_C = 0.02$), with a core-shell duplex grain structure. Alternatively, the enthalpy of grain boundary segregation of B could be positive, which changes the bond energy order in Equation 1 from $E_{AB}^{gb} > E_{AA/BB}^{gb}$ to $E_{AB}^{gb} < E_{AA/BB}^{gb}$:

$$E_{BC}^{gb} > E_{CC}^{gb} > \boldsymbol{E_{AA/BB}^{gb}} > \boldsymbol{E_{AB}^{gb}} > E_{AC/BC}^{c} > E_{CC}^{c} > E_{AB}^{c} > E_{AA/BB}^{c} > E_{AC}^{gb} \qquad (2)$$

This produces a microstructure without the "core-shell" grain structure, as shown in Figure 3(d) (ΔH_{AB}^{mix} is increased to $22 kJ/mol$), where the precipitates of B are now in direct contact with grain boundaries and in addition now interact with C. The lowest two

bond energies for each element are the same in both cases, and it is not until the 4th lowest bond energy of B is considered that the difference between these two classes of microstructure is explained: the bond energy orders for B become $E_{BB}^{c} < E_{AB}^{c} < E_{BC}^{c} < E_{AB}^{gb}$ (Figure 3(b)) instead of $E_{BB}^{c} < E_{AB}^{c} < E_{BC}^{c} < E_{BB}^{gb}$. Such a high bond energy becomes relevant in this situation because the presence of grain boundaries is imposed by solute C; thus the grain boundary bond energies (i.e. whether B segregates or anti-segregates) become relevant, whereas in a binary nanocrystalline alloy such a case cannot exist since the single solute element must stabilize the grain boundaries.

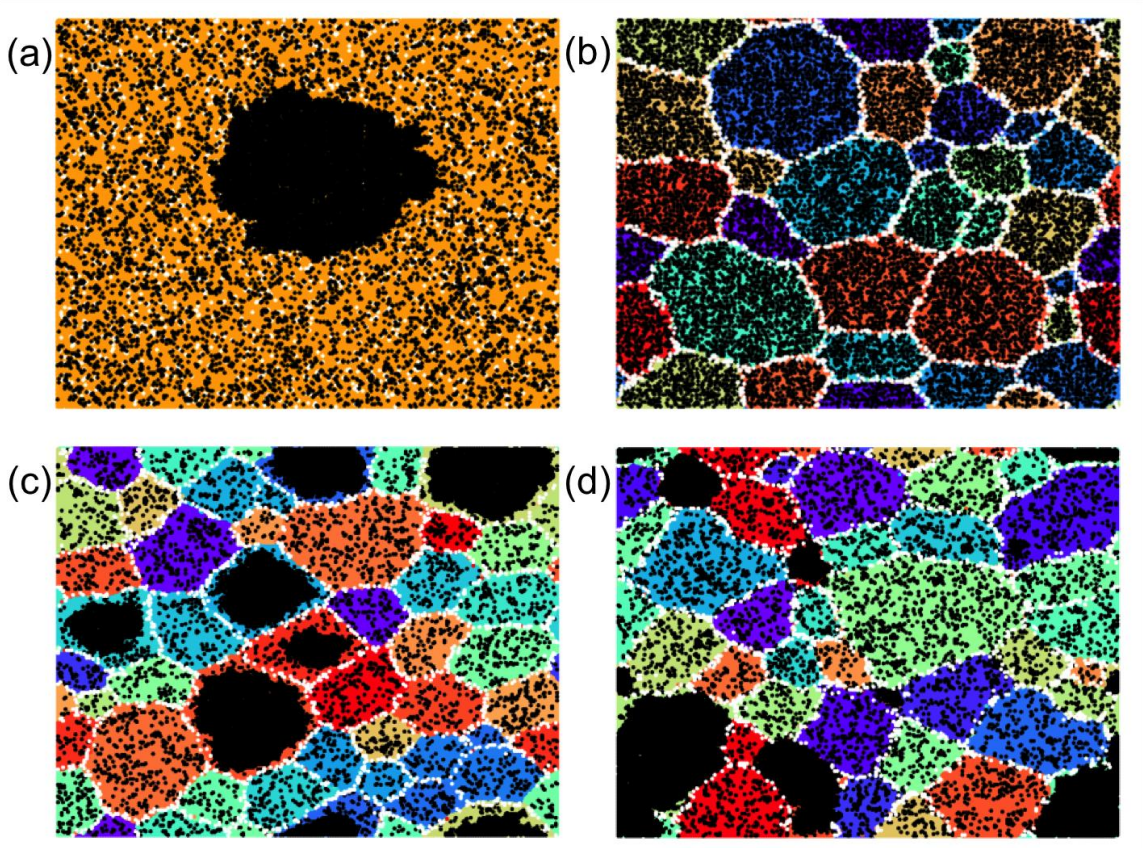

Figure 3. The microstructures of ternary systems with 20 at.% B (presented in black) and 2 at.% C (shown in white) at 500°C, and with different bond orders due to different

mixing enthalpies, where (a) and (b) are a result of 2nd rank variations of the system in Figure 2 (displayed in Figure 3(c)), and (d) is the result of a 4th rank variation. The corresponding bond energies are shown in Table 1.

In conclusion, we have evaluated the relative complexity and flexibility afforded in nanostructure design by traversing from simple binary to multicomponent systems. In ternary and higher order alloys, many unique microstructures are expected to become thermodynamically plausible, with complex topologies that are not amenable to simple mean-field or regular solution modeling. Combinations of elements with complementary roles in shaping the microstructure should open the door to new design strategies as well. Our Monte Carlo simulations herein show a few interesting examples from among the many thousand that are nominally possible, including core-shell grain boundary segregated states and dual-phase nano-duplex structures in which the length scale is set by the ternary addition. In light of the recent rising interest in impurity effects in nanostructured alloys [23,33,34,37,38], a simple non-regular multinary model such as the one presented here could provide significant insight on necessarily complex experiments in this space. It is hoped that future work can further develop the range of viable multinary nanostructures and seek them in the laboratory.

AUTHOR INFORMATION

Corresponding Author

* e-mail: schuh@mit.edu.

Author Contributions

The manuscript was written through contributions of all authors. All authors have given approval to the final version of the manuscript.

Notes

The authors declare no competing financial interest.

ACKNOWLEDGEMENTS

The authors are grateful for the financial support by U.S. Army Research Office under grant W911NF-14-1-0539 and through the Institute of Soldier Nanotechnologies at MIT. A.R.K. acknowledges a National Defense Science and Engineering Graduate Fellowship.

REFERENCES

[1] M. G. Kanatzidis, Semicond. Semimetals 69 (2000) 51.

[2] C. Uher, Semicond. Semimetals 69 (2000) 139.

[3] I. Terasaki, Y. Ishii, D. Tanaka, K. Takahata, Y. Iguchi, Japan Soc. Appl. Phys. 40 (2001) L65–L67.

[4] J. Bauer, M. Seeger, A. Zern, H. Kronmüller, J. Appl. Phys. 80 (1996) 1667–1673.

[5] T. Schrefl, J. Fidler, H. Kronmüller, Phys. Rev. B 49 (1994) 6100–6110.

[6] R. Fischer, T. Schrefl, H. Kronmüller, J. Fidler, J. Magn. Magn. Mater. 153 (1996) 35–49.

[7] T. Watanabe, S. Tsurekawa, Acta Mater. 47 (1999) 4171–4185.

[8] T. D. Shen, R. B. Schwarz, S. Feng, J. G. Swadener, J. Y. Huang, M. Tang, J. Zhang, S. C. Vogel, Y. Zhao, Acta Mater. 55 (2007) 5007–5013.

[9] S. Bechtle, M. Kumar, B. P. Somerday, M. E. Launey, R. O. Ritchie, Acta Mater. 57 (2009) 4148–4157.

[10] H. P. Chen, R. K. Kalia, E. Kaxiras, G. Lu, A. Nakano, K. I. Nomura, A. C. T. Van Duin, P. Vashishta, Z. Yuan, Phys. Rev. Lett. 104 (2010) 155502.

[11] J. Luo, H. Cheng, K. M. Asl, C. J. Kiely, M. P. Harmer, Science 333 (2011) 1730–1733.

[12] J. Weissmüller, Nanostructured Mater. 3 (1993) 261–272.

[13] A. J. Detor, C. A. Schuh, Acta Mater. 55 (2007) 371–379.

[14] P. Choi, T. Al-Kassab, F. Gärtner, H. Kreye, R. Kirchheim, Mater. Sci. Eng. A 353 (2003) 74–79.

[15] J. Weissrmuller, J. Mater. Res 9 (1994) 4.

[16] T. Chookajorn, H. A. Murdoch, C. A. Schuh, Science 337 (2012) 951–954.

[17] P. C. Millett, R. P. Selvam, A. Saxena, Acta Mater. 55 (2007) 2329–2336.

[18] P. Choi, M. Da Silva, U. Klement, T. Al-Kassab, R. Kirchheim, Acta Mater. 53 (2005) 4473–4481.

[19] K. A. Darling, B. K. VanLeeuwen, C. C. Koch, R. O. Scattergood, Mater. Sci. Eng. A 527 (2010) 3572–3580.

[20] E. Hondros, M. P. Seah, Phys. Metall. (1983) 856.

[21] B. Färber, E. Cadel, A. Menand, G. Schmitz, R. Kirchheim, Acta Mater. 48 (2000) 789–796.

[22] K. A. Darling, A. J. Roberts, Y. Mishin, S. N. Mathaudhu, L.J. Kecskes, J. Alloys Compd. 573 (2013) 142–150.

[23] N. Zhou, T. Hu, J. Huang, J. Luo, Scripta Mater. 124 (2016) 160–163.

[24] H. A. Murdoch, C. A. Schuh, Acta Mater. 61 (2013) 2121–2132.

[25] F. Liu, R. Kirchheim, J. Cryst. Growth 264 (2004) 385–391.

[26] A. R. Kalidindi, T. Chookajorn, C. A. Schuh, JOM 67 (2015) 2834–2843.

[27] M. Saber, H. Kotan, C. C. Koch, R. O. Scattergood, J. Appl. Phys. 114 (2013) 103510.

[28] T. Chookajorn, C. A. Schuh, Phys. Rev. B 89 (2014) 064102.

[29] A. J. Detor, C. A. Schuh, Acta Mater. 55 (2007) 4221–4232.

[30] F. Liu, R. Kirchheim, Scripta Mater. 51 (2004) 521–525.

[31] T. Chookajorn, C. A. Schuh, Acta Mater. 73 (2014) 128–138.

[32] M. Park, C. A. Schuh, Nat. Commun. 6 (2015) 6858.

[33] B. G. Clark, K. Hattar, M. T. Marshall, T. Chookajorn, B. L. Boyce, C. A. Schuh, JOM 68 (2016) 1625–1633.

[34] M. N. Polyakov, T. Chookajorn, M. Mecklenburg, C. A. Schuh, A. M. Hodge, Acta Mater. 108 (2016) 8–16.

[35] T. Chookajorn, M. Park, C. A. Schuh, J. Mater. Res. 30 (2015) 151–163.

[36] A. R. Kalidindi, C. A. Schuh, Comput. Mater. Sci. 118 (2016) 172–179.

[37] N. Argibay, T. A. Furnish, B. L. Boyce, B. G. Clark, M. Chandross, Scripta Mater. 123 (2016) 26–29.

[38] C. J. Marvel, D. Yin, P. R. Cantwell, M. P. Harmer, Mater. Sci. Eng. A 664 (2016)

49–57.